

SUPPLEMENTARY INFORMATION

Towards a Structure-Based Exciton Hamiltonian for the CP29 Antenna of Photosystem II

Frank Müh*, Dominik Lindorfer, Marcel Schmidt am Busch, and Thomas Renger

Institute for Theoretical Physics, Johannes Kepler University Linz, Altenberger Str. 69, 4040 Linz, Austria.

** E-mail: frank.mueh@jku.at*

ESI Text

Simulation of Linear Optical Spectra

The Hamiltonian underlying our simulations reads¹

$$H = H_{\text{Chl}} + H_{\text{Chl-Chl}} + H_{\text{Chl-rad}} + H_{\text{Chl-prot}} + H_{\text{prot}} \quad (8)$$

The first part contains the energies of electronic and vibrational states of the individual Chls

$$H_{\text{Chl}} = \sum_{m=1}^{13} \left(E_m |m 0\rangle \langle m 0| + \sum_{i=1}^{10} (E_m + \hbar\omega_i) |m 1_i\rangle \langle m 1_i| \right) \quad (9)$$

where m counts the Chl sites in CP29 and E_m is the site energy. In addition to the excited state $|m 0\rangle$, where no intramolecular vibrational mode of the Chl is excited, ten states $|m 1_i\rangle$ are assigned to each site that represent the first excited states of intramolecular vibrational modes i with frequency ω_i in the first excited electronic state of pigment m . The frequencies of these modes are 100, 175, 250, 300, 375, 500, 600, 725, 800, and 875 cm^{-1} and are assumed to be site-independent and to be the same for Chl a and Chl b . Thus, they do not represent exactly the normal mode vibrations of the Chls, but are meant to be effective modes that serve to complete the optical line shape. The frequencies ω_i and Huang-Rhys factors pertaining to these effective modes are inferred from a comparison of simulated and measured (disorder-averaged) fluorescence spectra of trimeric LHCII as described¹ and are assumed here to be a likewise valid approximation for the Chls in CP29. Note that it is sufficient to consider only one vibrational excitation in each mode because of the small Huang-Rhys factors (see ref. 1). The present treatment of intramolecular pigment modes is a compromise between neglecting them altogether² and including them into the spectral density of exciton-vibrational coupling³ (i.e., into $H_{\text{Chl-prot}}$, see below). While the former approach resulted in unsatisfactory optical line shapes for LHCII,² the latter yields difficulties in an approximate treatment of exciton dynamics and EET as discussed¹ (see also the discussion by Novoderezhkin *et al.*⁴).

The second part of the Hamiltonian in eq. (8) comprises the interactions between Q_Y transitions on different Chls:

$$H_{\text{Chl-Chl}} = \frac{1}{2} \sum_{m \neq n} \left(V_{mn} |m 0\rangle \langle n 0| + \sum_j V_{mj} \frac{FC_j(0,1)}{FC_j(0,0)} |m 0\rangle \langle n 1_j| + \sum_{i,j} V_{mn} \frac{FC_i(0,1) FC_j(0,1)}{FC_i(0,0) FC_j(0,0)} |m 1_i\rangle \langle n 1_j| + \text{h.c.} \right) \quad (10)$$

where $FC_i(0,0)$ and $FC_i(0,1)$ are the Franck-Condon factors for the 0-0 and 0-1 transition, respectively. Note that in eq. (10), the index i counts the modes of pigment m and the index j those of pigment n . The excitonic coupling is actually given by

$$V_{mn} = \tilde{V}_{mn} \prod_i |FC_i(0,0)|^2 \quad (11)$$

Here, the index i counts the equivalent modes of both pigments m and n and \tilde{V}_{mn} is the purely electronic coupling between the transition densities of the two pigments. In their extrapolation of vacuum transition dipole strengths, Knox and Spring⁵ analyzed only those parts of the experimental spectra that do not encompass the high-frequency vibrational modes, so that the factor $\prod_i |FC_i(0,0)|^2$ is already

accounted for in their values. Thus, scaling of computed transition densities according to eq. (4) ultimately yields the correct V_{mn} according to eq. (11). In eq. (10), the first and third term on the r.h.s describe interactions between 0-0 and 0-1 transitions, respectively, on different Chls, while the second term represents inter-pigment interactions of 0-0 and 0-1 transitions.

A problem in the calculation of optical spectra and excitation energy transfer in PPCs is that the dynamical localization of exciton states, i.e., the fast decay of coherences between local excited states due to coupling to protein vibrations, can not be modeled exactly within the present approach. Note that because of this dynamical localization, even weakly coupled transitions with close energies, that in an exciton picture may be delocalized, in fact become quickly localized. To model the dynamic localization of excitons implicitly, domains of strongly coupled pigments are introduced as discussed earlier.^{1, 2, 6} In this approximation, the exciton Hamiltonian $H_{\text{ex}} = H_{\text{Chl}} + H_{\text{Chl-Chl}}$ is partitioned into blocks in a way that the off-diagonal elements between different blocks (domains) are smaller than a certain threshold value V_c . Exciton delocalization is allowed only within domains. In earlier work,^{2, 7} we found $V_c = 20 \text{ cm}^{-1}$ to be a suitable value for simulating linear optical spectra of LHCII. Here, we adopt the same value for the homologous CP29. Within each domain (labeled with index α), the one-exciton eigenstates labeled with quantum number M_α are, in general, linear combinations of local excited states labeled m_α with the exciton coefficients $c_{m_\alpha}^{(M_\alpha)}$ characterizing the contribution of state m_α to eigenstate M_α (see below).

The small Franck-Condon factors of the 0-1 transitions cause any couplings between such transitions or between 0-1 and 0-0 transitions to be strongly reduced, so that they fall into the category of weak couplings ($V_{mn} < V_c$) that are set to zero in the calculation of exciton wave functions in order to restrict exciton delocalization to the domains. In other words, these weak couplings do not contribute to the exciton coefficients $c_{m_\alpha}^{(M_\alpha)}$. As a consequence, exciton localization occurs effectively only between 0-0 transitions. This approximation hinges on the weak Franck-Condon factors $FC_i(0,1)$ and appears to be a reasonable approximation for Chls, but it may fail for other types of pigments such as carotenoids. Therefore, we rigorously leave out the second and third term on the r.h.s. of eq. (10) in the calculation of domain eigenstates. Thus, the exciton Hamiltonian can be rewritten as

$$\begin{aligned}
H_{\text{ex}} = & \sum_{\alpha} \left(\sum_{M_\alpha} \varepsilon_{M_\alpha} |M_\alpha 0\rangle \langle M_\alpha 0| + \sum_{m_\alpha} \sum_i (E_{m_\alpha} + \hbar\omega_i) |m_\alpha 1_i\rangle \langle m_\alpha 1_i| \right) \\
& + \frac{1}{2} \sum_{\beta \neq \alpha} \sum_{\substack{m_\alpha, n_\beta \\ V_{m_\alpha n_\beta} < V_c}} \left(V_{m_\alpha n_\beta} |m_\alpha 0\rangle \langle n_\beta 0| + \sum_j V_{m_\alpha n_\beta} \frac{FC_j(0,1)}{FC_j(0,0)} |m_\alpha 0\rangle \langle n_\beta 1_j| \right. \\
& \left. + \sum_{i,j} V_{m_\alpha n_\beta} \frac{FC_i(0,1) FC_j(0,1)}{FC_i(0,0) FC_j(0,0)} |m_\alpha 1_i\rangle \langle n_\beta 1_j| + \text{h.c.} \right)
\end{aligned} \tag{12}$$

where the indices α and β count the domains and M_α labels the exciton states in domain α . The states $|M_\alpha 0\rangle$ are linear combinations of local excited states $|m_\alpha 0\rangle$ of the respective domain according to

$$|M_\alpha 0\rangle = \sum_{m_\alpha} c_{m_\alpha}^{(M_\alpha)} |m_\alpha 0\rangle \tag{13}$$

The ε_{M_α} in eq. (12) are the energies of delocalized zero-zero excited states of domain α . In the calculation of linear optical spectra, only the first sum over α in eq. (12) is relevant, whereas the remaining terms are negligible, but become operative in the simulation of slow inter-domain EET.¹

The third part of the Hamiltonian in eq. (8) describes the coupling of electronic and vibronic transitions of the Chls to the external light field in the rotating wave approximation:^{1, 8}

$$H_{\text{Chl-rad}} = A_{\omega} \mathbf{e} e^{-i\omega t} \sum_{m=1}^{13} \boldsymbol{\mu}_m \left(|m 0\rangle \langle 0 0| + \sum_{i=1}^{10} \frac{FC_i(0,1)}{FC_i(0,0)} |m 1_i\rangle \langle 0 0| + \text{h.c.} \right) \quad (14)$$

where we have disregarded the distinction between domains for brevity and $|0 0\rangle$ represents the state with all pigments m in their electronic ground state and none of the intramolecular modes excited. In eq. (14), A_{ω} is the amplitude of the external light field with frequency ω and polarization vector \mathbf{e} , and $\boldsymbol{\mu}_m$ is the transition dipole moment of the local Q_Y transition of pigment m . The magnitude of $\boldsymbol{\mu}_m$ is chosen as that of a Chl in a medium with refractive index n , which for $n^2 = 2.0$ is 5.47 D for Chl a and 4.61 D for Chl b .⁵ Note that by analogy to eq. (11)

$$\boldsymbol{\mu}_m = \tilde{\boldsymbol{\mu}}_m \prod_i FC_i(0,0) \quad (15)$$

where $\tilde{\boldsymbol{\mu}}_m$ is the purely electronic transition dipole moment. The direction of $\boldsymbol{\mu}_m$ is along the axis joining the nitrogen atoms N_B and N_D of the respective Chl according to the crystallographer's atom labeling scheme.

The remaining parts of the Hamiltonian in eq. (8) are given by

$$H_{\text{prot}} = T_{\text{nucl}} + \sum_{\xi} \frac{\hbar\omega_{\xi}}{4} Q_{\xi}^2 \quad (16)$$

$$H_{\text{Chl-prot}} = \sum_{m=1}^{13} \sum_{\xi} \hbar\omega_{\xi} Q_{\xi} g_{\xi}^{(m)} \left(|m 0\rangle \langle m 0| + \sum_{i=1}^{10} |m 1_i\rangle \langle m 1_i| \right) \quad (17)$$

Here, H_{prot} comprises a set of independent harmonic oscillators ξ with frequency ω_{ξ} representing the protein vibrations, and T_{nucl} is the kinetic energy of these oscillators. Q_{ξ} is a dimensionless normal mode coordinate. The coupling of these normal modes to the pigment transitions is characterized by a set of dimensionless coupling constants $g_{\xi}^{(m)}$. The exciton-vibrational coupling constants are subsumed in the spectral density^{9, 10}

$$J_{mn}(\omega) = \sum_{\xi} g_{\xi}^{(m)} g_{\xi}^{(n)} \delta(\omega - \omega_{\xi}) \quad (18)$$

which describes for $m = n$ the fluctuation of the site energy of pigment m and for $m \neq n$ the correlation in site energy fluctuations between pigments m and n . The actual dependence of $J_{mn}(\omega)$ on the site m is not known and probably small. Therefore, $J_{mn}(\omega)$ is approximated by an m -independent analytic function $J(\omega) = S_0 J_0(\omega)$ with

$$J_0(\omega) = \frac{1}{s_1 + s_2} \sum_{k=1}^2 \frac{s_k}{7! 2\omega_k^4} \omega^3 e^{-(\omega/\omega_k)^{1/2}} \quad (19)$$

containing the parameters $s_1 = 0.8$, $s_2 = 0.5$, $\hbar\omega_1 = 0.56 \text{ cm}^{-1}$, $\hbar\omega_2 = 1.94 \text{ cm}^{-1}$, and the Huang-Rhys factor $S_0 = 0.5$ also used earlier for LHCII.^{1, 2} The effect of correlations is modeled by introducing a correlation radius R_c of protein vibrations and setting

$$J_{mn}(\omega) = S_0 J_0(\omega) e^{-R_{mn}/R_c} \quad (20)$$

where R_{mn} is the distance between the centers of pigments m and n . The functional form of $J_0(\omega)$ has been derived from simulations⁸ of fluorescence line-narrowing spectra of the B777 complex¹¹ originating from light-harvesting complexes of purple bacteria.¹² Therefore, it has recently been baptized the “B777 spectral density”, and it was shown to be adequate for CP29 based on an analysis of difference fluorescence line-narrowing spectra.¹³ Solving the equation of motion for the reduced density matrix with H_{ex} as the relevant system,^{1, 8} the homogeneous line shape function of intra-Chl vibronic transitions follows as

$$D(\omega - \omega_{m,i}) = \frac{1}{2\pi} \int_{-\infty}^{\infty} dt e^{i(\omega - \omega_{m,i})t} e^{G(t) - G(0)} \quad (21)$$

where the transition frequency is given by

$$\omega_{m,i} = (E_m + \hbar\omega_i - \lambda)/\hbar \quad (22)$$

with the reorganization energy of protein modes

$$\lambda = \int_{-\infty}^{\infty} d\omega \hbar\omega J(\omega) \quad (23)$$

The function $G(t)$ is obtained from the spectral density $J(\omega)$ and the Bose-Einstein distribution function.^{1, 8, 9} The line shape function of zero-phonon exciton transitions is given by

$$D_M(\omega - \tilde{\omega}_M) = \frac{1}{2\pi} \int_{-\infty}^{\infty} dt e^{i(\omega - \tilde{\omega}_M)t} e^{G_M(t) - G_M(0)} e^{-|t|/\tau_M} \quad (24)$$

where $G_M(t) = \gamma_{MM} G(t)$ and γ_{MM} depends on the exciton coefficients $c_m^{(M)}$ as well as the correlation radius of protein vibrations R_c . The latter was chosen to be $R_c = 5 \text{ \AA}$.¹⁴ In eq. (24), τ_M is the lifetime of exciton state $|M 0\rangle$ determined by exciton relaxation, and $\hbar\tilde{\omega}_M$ is shifted with respect to the exciton state energy ϵ_M in eq. (12) by reorganization effects due to coupling to the protein modes.^{2, 8}

The absorbance spectrum of the PPC is given as the sum of disorder-averaged spectra of the domains[†]

$$\text{OD}(\omega) \propto \sum_{\alpha} \omega \left\langle \sum_{M_{\alpha}} |\mu_{M_{\alpha}}|^2 D_{M_{\alpha}}(\omega - \tilde{\omega}_{M_{\alpha}}) + \sum_{m_{\alpha}} |\mu_{m_{\alpha}}|^2 \sum_i \frac{|FC_i(0,1)|^2}{|FC_i(0,0)|^2} D(\omega - \omega_{m_{\alpha},i}) \right\rangle_{\text{dis}} \quad (25)$$

Here, the transition dipole moments of the delocalized exciton states are linear combinations of the local transition dipole moments

$$\mu_{M_{\alpha}} = \sum_{m_{\alpha}} c_{m_{\alpha}}^{(M_{\alpha})} \mu_{m_{\alpha}} \quad (26)$$

The disorder average indicated by $\langle \dots \rangle_{\text{dis}}$ in eq. (25) is performed by a Monte-Carlo procedure, where each of the 13 site energies is varied randomly according to a Gaussian distribution with center E_m and

[†] Note that there is a misprint in the corresponding formulae in ref. 7, where $|FC_i(0,1)|^2 / |FC_i(0,0)|^2$ is replaced with $|FC_i(0,1)|^2$.

width $\sigma = 130 \text{ cm}^{-1}$. The value of σ is inferred from a comparison of simulated and measured spectra. In the calculation of LD spectra, the squares of transition dipole moments $|\boldsymbol{\mu}_{(M_\alpha, m_\alpha)}|^2$ in eq. (25) are replaced with $|\boldsymbol{\mu}_{(M_\alpha, m_\alpha)}|^2 (1 - 3 \cos^2 \theta_{(M_\alpha, m_\alpha)})$, where $\theta_{(M_\alpha, m_\alpha)}$ is the angle between the vector $\boldsymbol{\mu}_{(M_\alpha, m_\alpha)}$ and the membrane normal. Since exciton delocalization is considered here only between zero-zero intramolecular vibronic transitions, the CD spectra are calculated by

$$\text{CD}(\omega) \propto \sum_{\alpha} \left\langle \sum_{M_\alpha} R_{M_\alpha} D_{M_\alpha}(\omega - \tilde{\omega}_{M_\alpha}) \right\rangle_{\text{dis}} \quad (27)$$

with the rotational strength

$$R_{M_\alpha} = \sum_{m_\alpha, n_\alpha} c_{m_\alpha}^{(M_\alpha)} c_{n_\alpha}^{(M_\alpha)} E_{m_\alpha} \mathbf{R}_{m_\alpha n_\alpha} \cdot (\boldsymbol{\mu}_{m_\alpha} \times \boldsymbol{\mu}_{n_\alpha}) \quad (28)$$

The vector $\mathbf{R}_{m_\alpha n_\alpha} = \mathbf{R}_{m_\alpha} - \mathbf{R}_{n_\alpha}$ connects the centers of pigments m and n in domain α .

In the simulation of fluorescence spectra

$$I(\omega) = \langle I_{\text{hom}}(\omega) \rangle_{\text{dis}} \quad (29)$$

a thermal relaxation of the excitation energy in the excited states of the PPC is assumed to have taken place prior to fluorescence.^{8, 15} Assuming negligible thermal population of intramolecular pigment modes, the homogeneous fluorescence spectrum $I_{\text{hom}}(\omega)$ follows as:¹

$$I(\omega) \propto \omega^3 \sum_{\alpha} \sum_{M_\alpha} f(M_\alpha) \left\{ |\boldsymbol{\mu}_{M_\alpha}|^2 D_{M_\alpha}(\tilde{\omega}_{M_\alpha} - \omega) + \sum_{m_\alpha} |\boldsymbol{\mu}_{m_\alpha}|^2 |c_{m_\alpha}^{(M_\alpha)}|^2 \sum_i \frac{|FC_i(0,1)|^2}{|FC_i(0,0)|^2} D(\omega_{M_\alpha, m_\alpha, i} - \omega) \right\} \quad (30)$$

Here, the emission line shape functions $D_{M_\alpha}(\tilde{\omega}_{M_\alpha} - \omega)$ and $D(\omega_{M_\alpha, m_\alpha, i} - \omega)$ are obtained from eqs. (24) and (21) by replacing $\omega - \tilde{\omega}_M$ with $\tilde{\omega}_{M_\alpha} - \omega$ and $\omega - \omega_{m,i}$ with $\omega_{M_\alpha, m_\alpha, i} - \omega$, respectively, where $\omega_{M_\alpha, m_\alpha, i}$ is the frequency of the transition from state $|M_\alpha 0\rangle$ to the state, in which pigment m_α is in its electronic ground state with one vibrational excitation in mode i and all other pigments are in their electronic and vibrational ground states. The Boltzmann factor $f(M_\alpha)$ describes a thermal population of states $|M_\alpha 0\rangle$ with energies ε_{M_α} taking into account all domains:

$$f(M_\alpha) = \frac{e^{-\varepsilon_{M_\alpha}/k_B T}}{\sum_{\alpha} \sum_{M_\alpha} e^{-\varepsilon_{M_\alpha}/k_B T}} \quad (31)$$

ESI Tables

Table 5: Excitonic couplings (cm^{-1}) between Chl sites m and n in CP29 obtained by using the Poisson-TrEsp method based on HF-CIS.

m	n												
		3	4	6	7	8	9	10	11	12	13	14	15
2		13	5	4	5	-7	-25	-5	0	7	0	1	40
3		-	1	-2	5	4	103	7	-1	1	2	-3	-2
4			-	66	24	-4	-3	0	-4	3	2	-2	-3
6				-	15	-4	5	0	-2	1	1	-1	-2
7					-	-3	-2	0	-2	2	3	-1	-2
8						-	29	49	5	-1	-2	1	6
9							-	-1	5	-1	-3	1	6
10								-	-31	13	5	0	-10
11									-	95	-2	0	85
12										-	2	1	-1
13											-	-21	-3
14												-	0

Table 6: Calculated site energy shifts ΔE_m for the Chls in CP29 (cm^{-1}) using atomic partial charges from different quantum chemical methods as indicated based on the PBQC ($\tilde{\epsilon}_p = 1.8$, $\epsilon_{\text{mem}} = 2.0$, $\epsilon_{\text{solv}} = 5.0$) or the CDC method ($\epsilon_{\text{eff}} = 2.0$).

m	PBQC			CDC		
	BHHLYP	B65LYP	HF-CIS	BHHLYP	B65LYP	HF-CIS
2	-151	-138	-123	-120	-100	-72
3	-4	-13	-15	30	17	73
4	-91	-63	-73	-147	-91	-84
6	-113	-80	-48	-89	-36	25
7	-64	-51	-25	-106	-67	-3
8	-227	-230	-235	-257	-230	-210
9	35	16	35	35	20	64
10	-42	-19	-3	0	31	84
11	-286	-250	-144	-245	-199	-61
12	39	47	-2	67	81	71
13	-59	-55	-53	-69	-51	-9
14	-2	10	8	-5	31	61
15	-111	-94	19	-135	-118	22

Table 7. Standard deviations (cm^{-1}) between calculated and fitted site energies for CP29; for correlation plots, see Figure 9.

	BHHLYP	B65LYP	HF-CIS
PBQC	112	107	90
CDC	99	98	85

Table 8. Contribution of selected amino acid residues and cofactors to the site energy shift ΔE_2 (cm^{-1}) of Chl *a*602 in CP29 (pdb 3PL9) calculated with CDC using charge sets based on three different quantum chemical methods compared to those of homologous groups in LHCII (pdb 1RWT) calculated with HF-CIS charge sets. $\epsilon_{\text{eff}} = 2.0$.

group	CP29						LHCII	
	ΔE_2						group	ΔE_2
	complete residue			side chain			complete residue ^a	
	BHHLYP	B65LYP	HF-CIS	BHHLYP	B65LYP	HF-CIS		HF-CIS
Gly 88	-3	2	2	-	-	-	Thr 57	8
Leu 89	11	10	12	2	1	1	Phe 58	8
Glu 90	-3	2	2	-7	-3	-3	Ala 59	4
Arg 91	-68	-78	-69	-79	-87	-79	Lys 60	-32
Phe 92	52	41	47	14	9	10	Asn 61	69
Arg 93	40	-1	17	31	-9	10	Arg 62	16
Glu 94	45	59	47	43	57	47	Glu 63	44
Cys 95	-30	-27	-36	-18	-15	-18	Leu 64	-22
Glu 96	-205	-132	-145	-192	-113	-118	Glu 65	-149
Leu 97	7	4	2	3	2	2	Val 66	0
Ile 98	-14	-14	-15	-1	-1	-1	Ile 67	-13
His 99	-28	-27	-26	-2	-2	-1	His 68	-21
Glu 100	-5	-6	-6	-7	-8	-1	Cys 69	-9
Arg 101	-22	-35	-16	-16	-29	-10	Arg 70	-15
Σ	-223	-202	-186	-229	-198	-161	Σ	-112

^a average of the three equivalent sites in the LHCII trimer.

Table 9. Contribution of selected amino acid residues and cofactors to the site energy shift ΔE_3 (cm^{-1}) of Chl *a*603 in CP29 (pdb 3PL9) calculated with CDC using charge sets based on three different quantum chemical methods compared to those of homologous groups in LHCII (pdb 1RWT) calculated with HF-CIS charge sets. $\epsilon_{\text{eff}} = 2.0$.

group	CP29						LHCII	
	ΔE_3						group	ΔE_3
	complete residue			side chain			complete residue ^a	
	BHHLYP	B65LYP	HF-CIS	BHHLYP	B65LYP	HF-CIS		HF-CIS
Gly 88	0	1	3	–	–	–	Thr 57	–2
Leu 89	–3	–1	–2	0	0	0	Phe 58	–1
Glu 90	–1	0	0	0	0	0	Ala 59	–1
Arg 91	14	–30	38	17	–28	41	Lys 60	23
Phe 92	–4	–2	–3	–3	–1	–2	Asn 61	–8
Arg 93	10	–7	10	11	–6	11	Arg 62	8
Glu 94	–25	–2	–36	–24	0	–34	Glu 63	–30
Cys 95	1	–4	–11	1	–2	–8	Leu 64	–2
Glu 96	–1	21	7	2	24	11	Glu 65	10
Leu 97	–1	–1	–2	–1	–1	–1	Val 66	–1
Ile 98	4	1	2	1	1	1	Ile 67	–1
His 99	–38	–26	–16	–44	–28	–17	His 68	–11
Glu 100	–1	–2	–3	–2	–1	–3	Cys 69	–1
Arg 101	25	8	32	21	6	29	Arg 70	31
Σ	–20	–44	19	–21	–36	28	Σ	14

^a average of the three equivalent sites in the LHCII trimer.

ESI Figures

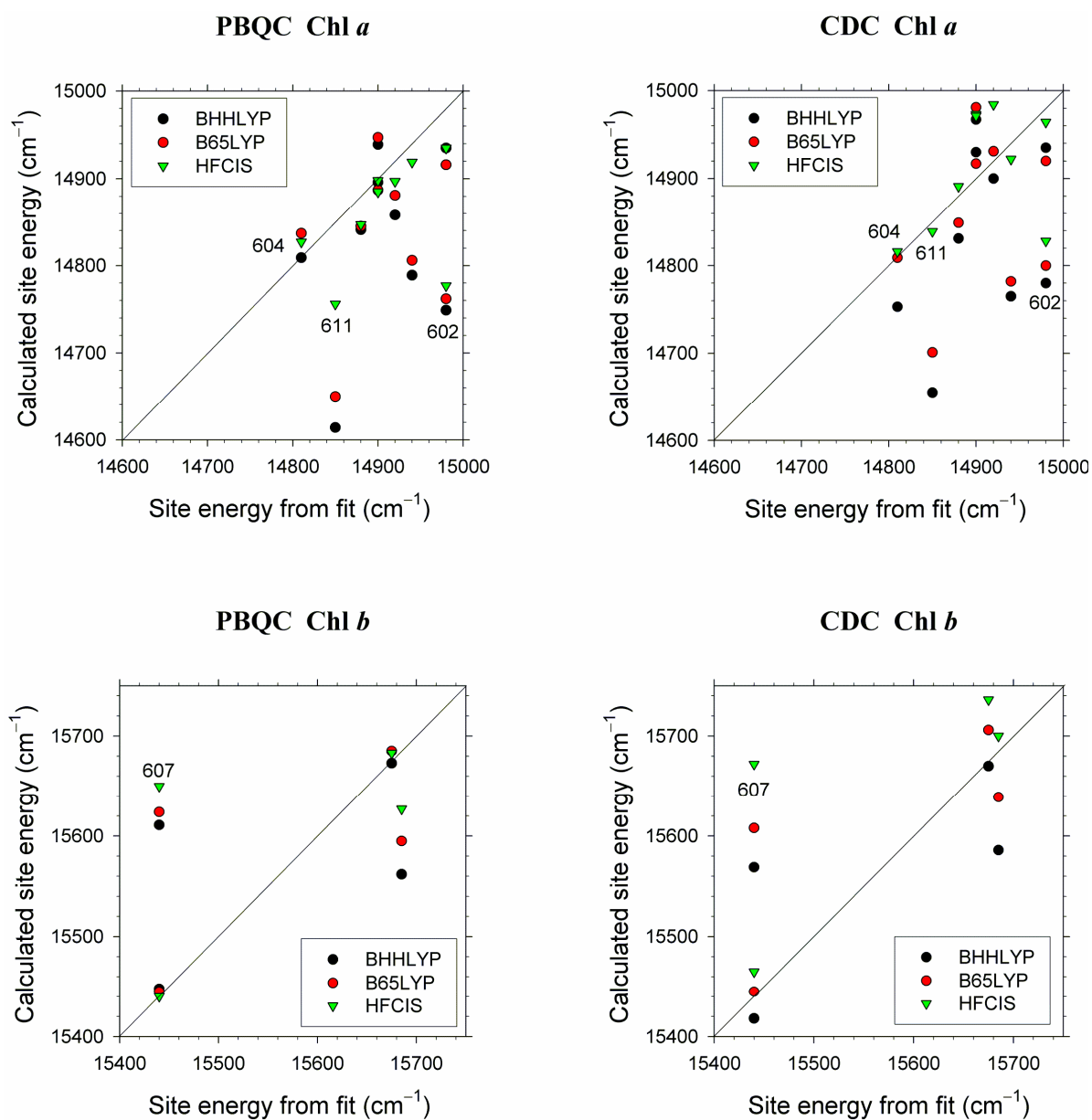


Figure 9.

Correlation of calculated and fitted site energies of Chl *a* (top) and Chl *b* (bottom) sites in CP29 for different quantum chemical methods used to calculate atomic partial charges, employing either the PBQC method (left) or the CDC method (right). Standard deviations are listed in Table 7.

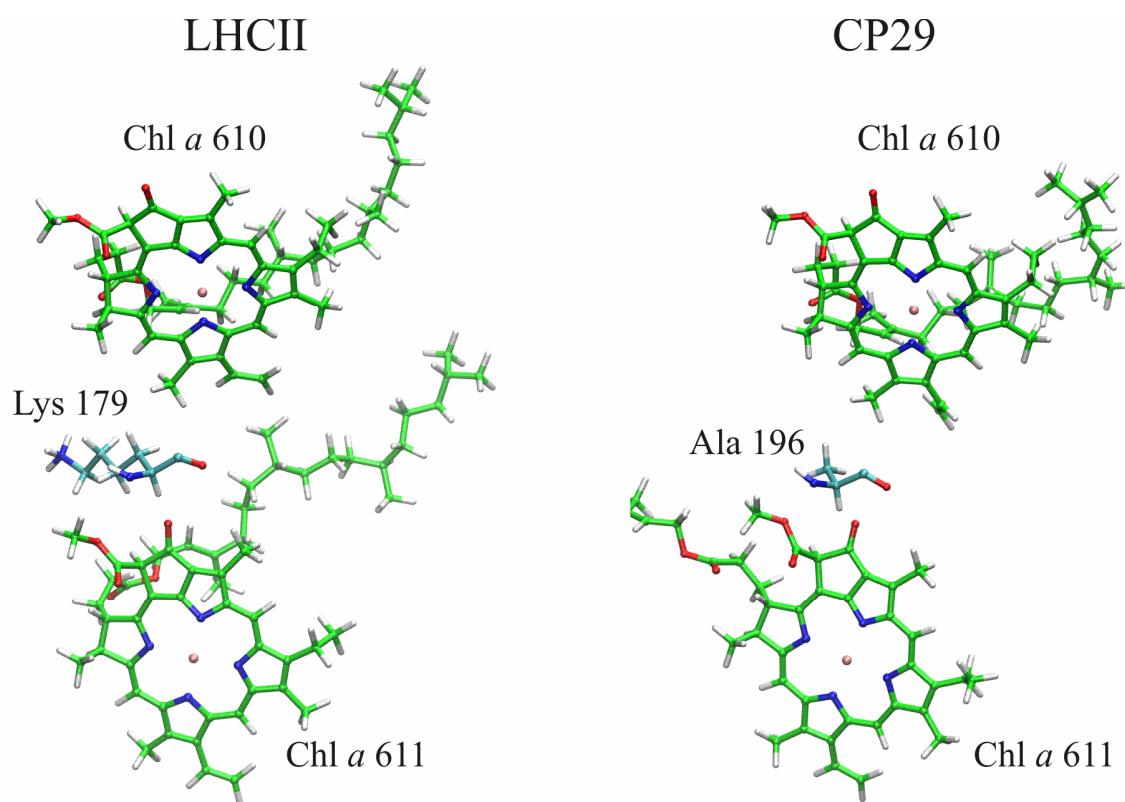


Figure 10. *Left:* Lys 179 located between Chl *a*610 and *a*611 in LHCII (PDB 1RWT¹⁶). *Right:* Ala 196 in CP29, which is homologous to Lys 179 in LHCII, located between Chl *a*610 and *a*611 (PDB 3PL9¹⁷). Figures made with VMD.¹⁸

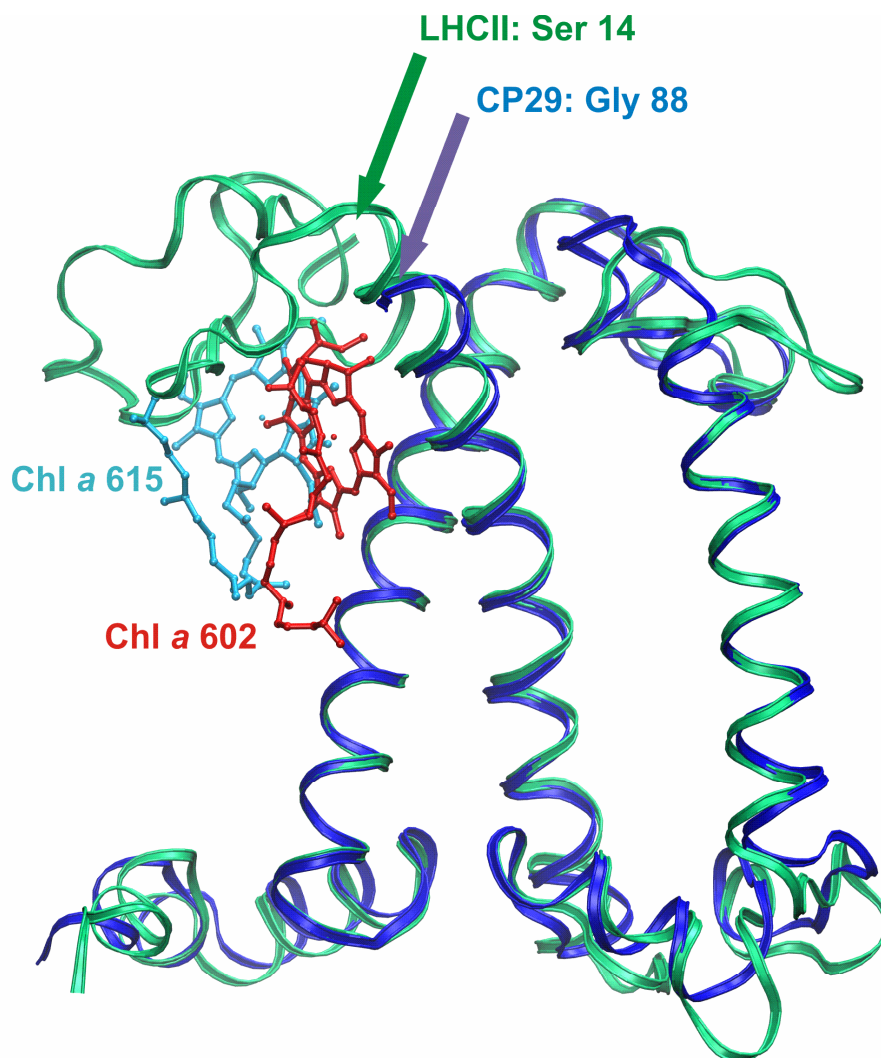


Figure 11. Overlay of the peptide backbone structures of CP29 (blue; PDB 3PL9¹⁷) and LHCII (green; PDB 1RWT¹⁶). The indicated amino acid residues are the first in the sequence modeled in the crystal structure: Gly 88 in CP29 (which is homologous to Thr 57 in LHCII) and Ser 14 in LHCII. Note that a significant portion of the N-terminus is missing in CP29. Also shown are Chls *a*602 (red) and *a*615 (cyan) of CP29 to indicate their position relative to the missing N-terminus. Overlay and figure made with VMD.¹⁸

ESI References

1. T. Renger, M. E. Madjet, A. Knorr and F. Müh, *J. Plant Physiol.*, 2011, **168**, 1497-1509.
2. F. Müh, M. E. A. Madjet and T. Renger, *J. Phys. Chem. B*, 2010, **114**, 13517-13535.
3. V. I. Novoderezhkin, M. A. Palacios, H. van Amerongen and R. van Grondelle, *J. Phys. Chem. B*, 2005, **109**, 10493-10504.
4. V. Novoderezhkin, A. Marin and R. van Grondelle, *Phys. Chem. Chem. Phys.*, 2011, **13**, 17093-17103.
5. R. S. Knox and B. Q. Spring, *Photochem. Photobiol.*, 2003, **77**, 497-501.
6. F. Müh, T. Renger and A. Zouni, *Plant Physiol. Biochem.*, 2008, **46**, 238-264.
7. F. Müh and T. Renger, *Biochim. Biophys. Acta*, 2012, **1817**, 1446-1460.
8. T. Renger and R. A. Marcus, *J. Chem. Phys.*, 2002, **116**, 9997-10019.
9. T. Renger and F. Müh, *Phys. Chem. Chem. Phys.*, 2013, **15**, 3348-3371.
10. T. Renger, M. E. Madjet, M. Schmidt am Busch, J. Adolphs and F. Müh, *Photosynth. Res.*, 2013, **116**, 367-388.
11. T. M. H. Creemers, C. A. De Caro, R. W. Visschers, R. van Grondelle and S. Völker, *J. Phys. Chem. B*, 1999, **103**, 9770-9776.
12. P. S. Parkes-Loach, J. R. Sprinkle and P. A. Loach, *Biochemistry*, 1988, **27**, 2718-2727.
13. A. Kell, X. M. Feng, M. Reppert and R. Jankowiak, *J. Phys. Chem. B*, 2013, **117**, 7317-7323.
14. T. Renger, *Photosynth. Res.*, 2009, **102**, 471-485.
15. G. Raszewski and T. Renger, *J. Am. Chem. Soc.*, 2008, **130**, 4431-4446.
16. Z. F. Liu, H. C. Yan, K. B. Wang, T. Y. Kuang, J. P. Zhang, L. L. Gui, X. M. An and W. R. Chang, *Nature*, 2004, **428**, 287-292.
17. X. W. Pan, M. Li, T. Wan, L. F. Wang, C. J. Jia, Z. Q. Hou, X. L. Zhao, J. P. Zhang and W. R. Chang, *Nat. Struct. Mol. Biol.*, 2011, **18**, 309-315.
18. W. Humphrey, A. Dalke and K. Schulten, *J. Mol. Graphics*, 1996, **14**, 33-38.